Physics Letters B 831 (2022) 137145

Contents lists available at ScienceDirect

Physics Letters B

www.elsevier.com/locate/physletb

Isospin dependence of nuclear level density at A≈ 120 mass region

R. Shil [a], K. Banerjee [b,c,*], Pratap Roy [b,c,1], J. Sadhukhan [b,c], T.K. Rana [b,c], G. Mukherjee [b,c], S. Kundu [b,c], T.K. Ghosh [b,c], S. Manna [b,c], A. Sen [b,c], R. Pandey [b], A. Chakraborty [a], Deepak Pandit [b,c], S. Mukhopadhyay [b,c], Debasish Mondal [b,c], D. Paul [b,c], C. Bhattacharya [b,c], S. Bhattacharya [b,2]

[a] Department of Physics, Siksha Bhavana, Visva-Bharati, Santiniketan 731235, India
[b] Variable Energy Cyclotron Centre, 1/AF, Bidhan Nagar, Kolkata 700064, India
[c] Homi Bhabha National Institute, Training School Complex, Anushakti Nagar, Mumbai 400094, India

ARTICLE INFO

Article history:
Received 5 January 2022
Received in revised form 23 April 2022
Accepted 29 April 2022
Available online 4 May 2022
Editor: D.F. Geesaman

Keywords:
Nuclear level density
Isospin dependence
Level density parameter
Statistical model

ABSTRACT

Nuclear level density and the level density parameter of ^{115,119,127}Te isotopes are experimentally determined by analyzing the backward angle neutron energy spectra from ^{4}He+^{112,116,124}Sn reactions. Measurements are done in the compound nuclear excitation energy range of 25-42 MeV. Statistical model analysis is performed to test different phenomenological prescriptions of the level density parameter. Our data efficiently scan the explicit dependences of level density on three key factors: nuclear deformation, neutron-proton asymmetry, and the separation from the most stable isobar. It is observed that the experimental data are best described when deviation in atomic number from the corresponding β-stable isobar is explicitly taken into account. Further, nuclear level densities determined from the measured spectra show a reduction for ^{115,127}Te in comparison to that of ^{119}Te, which lies closer to the β-stability line.

1. Introduction

Nuclear level density (NLD) governs the statistical decay of excited nuclei. Thus, it is an important input for the nuclear reaction codes. Over the years, significant amount of research are carried out to understand the dependency of NLD on various key factors such as excitation energy [1–5], angular momentum [4–7], nuclear shell structure [8–10], ground state deformation and associated collective enhancement [11–18], nucleonic pairing [19,20] etc. Several independent experimental techniques like the counting of nuclear levels, measurement of the neutron resonance spacing [21,22], and analysis of the primary gamma-ray (*Oslo Method*) [23–25] and particle evaporation spectra [26] are widely used to understand the nature of NLD as a function of the above-mentioned factors. One of the major issues that still needs attention is the dependence of NLD on the neutron (N)- proton (Z) asymmetry, which is commonly measured in terms of the isospin projection $(N-Z)/2$. This asymmetry is expected to hardly affect the nuclei around the valley of stability, but it could have profound impact on the neutron or proton rich nuclei. Although numerous theoretical [27–31] and experimental [2,32–35] investigations are pursued to study the isospin dependence, but a proper understanding of this phenomenon over a broader mass range is still missing. In particular, such variation of NLD along certain isotopic chains is crucial for quantitative understanding of several nuclear reactions pertinent to nuclear astrophysics.

The widely used theoretical expression for NLD was originally suggested by Bethe, who derived it by assuming the nucleus as a non interacting Fermi gas [36]. In this prescription [more details can be found in Appendix Eq. (A.1)], the level density parameter a, and its asymptotic value $\tilde{a}$ to be precise, is a crucial input that needs to be determined very accurately. Within the Fermi gas model, $\tilde{a}$ signifies the density of states at the Fermi energy, and it is often approximated as,

$$\tilde{a} = \alpha A, \tag{1}$$

where α is, in principle, a constant independent of the nucleus. However, from intuitive understanding, an explicit dependence on N and Z is expected. To this end, alternative empirical formulae for $\tilde{a}$ were proposed by Al-Quraishi et al. [28,29]. They analysed the

* Corresponding author at: Variable Energy Cyclotron Centre, 1/AF, Bidhan Nagar, Kolkata 700064, India.
E-mail address: kaushik@vecc.gov.in (K. Banerjee).
[1] Presently at: GSI Helmholtzzentrum für Schwerionenforschung, D-64291 Darmstadt, Germany.
[2] Superannuated.

https://doi.org/10.1016/j.physletb.2022.137145

measured NLDs at low excitation energies $\sim$ up to 8 MeV in the mass region of $20 < A < 110$, and ended up with two preferred choices,

$$\tilde{a} = \frac{\alpha A}{\exp[\beta(N-Z)^2]}, \tag{2}$$

and

$$\tilde{a} = \frac{\alpha A}{\exp[\gamma(Z-Z_0)^2]}, \tag{3}$$

where β and γ are empirical constants, and Z_0 is the atomic number of the β-stable isobar situated at the bottom of the associated mass parabola. Z_0 can be estimated from Eq. (A.2) of the Appendix. Since Eq. (2) is directly connected to the isospin asymmetry $(N-Z)$, it may be more critical for exotic nuclei in the low mass region, where stable nuclei lies near the $N=Z$ line. On the other hand, the second formula gives stronger effects over the whole mass region when Z moves further away from the corresponding β-stable isobar. Both the aspects are crucial for nucleosynthesis calculations associated to *r*- and *rp*-processes. Therefore, it is extremely important to validate the above-mentioned empirical formulae through experiments.

Apart from the explicit N and Z dependences, it was recommended [12] that Eq. (1) can be improved by adding *surface* ($\propto A^{2/3}$) and *curvature* ($\propto A^{1/3}$) corrections. These additional terms take into account the effects due to nuclear ground-state deformation. The modified $\tilde{a}$ can be written as [12],

$$\tilde{a} = 0.04543 r_0^3 A + 0.1355 r_0^2 A^{2/3} B_s + 0.1426 r_0 A^{1/3} B_k, \tag{4}$$

where r_0 is the nuclear radius parameter. B_s and B_k are the coefficients appearing due to the ground state deformation. Usually, quadrupole moment is the dominant deformation mode at the ground state, and it can be represented with the Bohr's deformation parameter β_2. Expressions for B_s and B_k as a functions of β_2 are given in Eq. (A.3) in Appendix. A deformed nucleus generally exhibits collective enhancement over the single particle level density which is due to the low-energy collective states associated with small amplitude collective motions. Signature of collective enhancement has been seen in a number of recent measurements [13–18]. However, such effects do not hinder our search for isospin dependence in NLD as elaborated in Section 5. Also, the NLD parameter $\tilde{a}$ needs to be corrected for nuclear shell effect to get the shell corrected parameter a, which is incorporated here as described in Refs. [8].

In the last two decades, a few measurements were attempted to explore the isospin dependence of NLD in the mass region of $A > 110$ and at excitation energies above 8 MeV. In one of such studies, light particle spectra from the ^{60}Ni + ^{92,100}Mo reactions were measured in coincidence with the evaporation residues. No significant isospin dependence in NLD was observed [2]. Similar conclusion was drawn in the theoretical study by Charity and Sobotka [31]. In another experiment (^{32}S + ^{107}Ag) [32], somewhat better agreement was observed with Eq. (2); however, they could not provide a clear indication in favour of the $(N-Z)$ dependence. Further, in the above measurements, compound nuclei are populated using heavy-ion beams where the final outcomes are influenced by the large angular momenta, which in turn complicate the signature of individual effect like isospin.

There are renewed interests in the study of NLD triggered by recent measurements [33–35]. Particularly, evidences in support of the isospin dependent $\tilde{a}$ are observed. Also, in our last measurement [35], Eq. (3) was found to be more suitable to explain the evaporated neutron energy spectra in two isobars of A =115. As a continuation, in the present work, we investigate the properties of NLD by testing different forms of $\tilde{a}$ for the three residues, ^{115,119,127}Te populated via ^{4}He+^{112,116,124}Sn reactions with compound nuclear excitation energy (E^*_{CN}) in the range of 25-42 MeV.

2. Experimental details

The experiment was performed with the ^{4}He beam, having energy in the range of 26-44 MeV, from the K130 Cyclotron facility at VECC. Isotopically enriched ^{112,116,124}Sn targets of thickness 2.3, 2.0, and 2.5 mg/cm^2, respectively were placed inside a 3 mm thick stainless steel reaction chamber. Emitted neutrons were detected using four liquid scintillator based neutron detectors of dimensions $5'' \times 5''$ placed at the laboratory angles of 55°, 120°, 135°, and 150° at a distance of 1.5 m from the target.

Energies of the emitted neutrons were measured by the time-of-flight (TOF) technique. Each valid start of the TOF was generated from a 50-element BaF_2 gamma-ray detector array [37] when at least two detectors of the array fired simultaneously and was in coincidence with the OR signal generated from all the neutron detectors. The BaF_2 array was divided into two parts in a staggered-castle type geometry and was placed on the top and bottom sides of the reaction chamber. The neutron and gamma separation was achieved by both TOF and pulse shape discrimination using zero cross over (ZCO) measurements [38]. The pulse height (PH), ZCO time and TOF spectra were recorded on event by event basis using a VME based data acquisition system. The beam dump was kept at a distance of $\sim$3 m from the target position and was well shielded with the layers of lead and high density polyethylene (HDPE) for minimizing the contributions of background neutrons originated in the beam dump [39]. The pulse height spectra were calibrated using gamma-ray sources and the TOF was calibrated using the precision time calibrator.

3. Extracting evaporated neutron spectra

Typical two-dimensional spectrum comprising of ZCO and TOF are shown in Fig. 1(a) which indicates a clear separation between neutron and gamma events. The neutron TOF spectra were extracted from the ZCO vs TOF plot by projecting the recorded neutron events along the TOF axis. The TOF spectra were subsequently converted to neutron energy spectra by incorporating a Jacobian transformation [40] and taking the prompt gamma peak as the time reference. Further, the neutron energy spectra were corrected for the efficiency of the neutron detectors, which were measured using the same setup with a ^{252}Cf source placed at the target position. The contribution of the scattered neutrons from the surrounding estimated using a *shadow bar* comprising of HDPE blocks having thickness of 30 cm was subtracted from the measured data. The energy spectra thus obtained at the forward (55°) and backward (150°) angles for the ^{4}He + ^{116}Sn reaction at $E^*_{CN} = 39$ MeV are shown in Fig. 1(b).

3.1. Differentiating pre-equilibrium decay

The measured forward- and backward-angle spectra are compared with the calculated spectra [see Fig. 1(b)] to isolate the possible effect of pre-equilibrium contributions. The theoretical calculations were performed with the TALYS (v1.8) code [41]. In this calculation, we consider two different nuclear decay modes: (1) the pre-equilibrium decay and (2) the compound nuclear decay. In the TALYS calculations, contributions from (1) and (2) are estimated by employing the Exciton model [42,43] and the Hauser-Feshbach (HF) model [44], respectively. Fig. 1(b) shows that the backward angle data can be reproduced well with the mode (2) alone, whereas both the modes are required to explain the forward angle data. Following this observation, we henceforth use only the backward-angle data to study NLD.

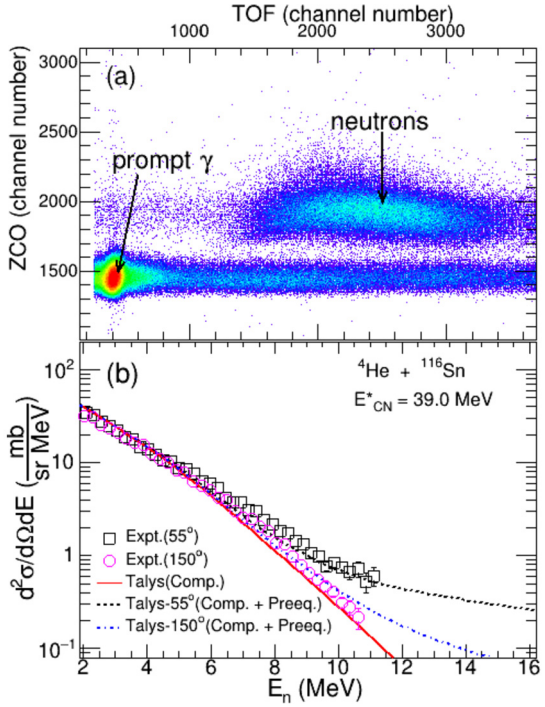

Fig. 1. (a) Typical Zero Cross Over vs Time of Flight spectra shows a clear separation between neutron and gamma events (b) Neutron energy spectra from the ^{4}He + ^{116}Sn reaction measured at forward (55°) (open squares) and backward (150°) (open circles) angles. Spectra calculated using the TALYS code considering compound (solid line) and compound + pre-equilibrium (dashed and dash dotted lines) reaction modes are also shown for comparison.

4. Analysis of neutron energy spectra

4.1. Benchmarking model parameters

Neutron spectra following compound nuclear decay calculated using the HF formalism required NLD which is calculated using the Back-shifted Fermi Gas (BSFG) model [45] (see Appendix). NLD parameter $\tilde{a}$ is required as a input in this calculation which can be estimated using any of the formulae described in Eqs. (1) to (4). For using Eqs. (1)-(3) we need to determine the constant α before proceeding further. To this end, we consider ^{4}He + ^{116}Sn as our reference reaction as the major residue ^{119}Te produced here (at lowest E^*_{CN}) lie closest to the beta stability line at $Z = 52$. It should be pointed out that the experimental neutron spectra contain contributions from different stages of the decay cascade. However, at the present E^*_{CN} the spectra are mostly determined by the first chance ($1n$) neutron emissions (see Section 4.2) leading to ^{115}Te, ^{119}Te and ^{127}Te as major residues for the reactions ^{4}He + ^{112}Sn, ^{116}Sn and ^{124}Sn, respectively. First, we calculate the spectra for ^{4}He + ^{116}Sn at the lowest E^*_{CN} by employing Eq. (1). Corresponding χ^2 between measured and calculated neutron spectra was minimized by varying α. The optimum value of α thus obtained is 0.109 ± 0.001, which is very close to the previous estimate of 0.107 [29]. The same value of α was used for the other two reactions and in Eqs. (2) and (3) as well.

For a given reaction, the coefficients β and γ appearing in Eqs. (2) and (3), are less sensitive compared to α. The values of β and γ were taken from Ref. [29]. In case of Eq. (4), the radius parameter r_0 was determined by fitting the measured spectra in ^{4}He + ^{124}Sn which is found to be 1.16 ± 0.01. In this reaction ^{127}Te is the most significant residue which is nearly spherical making Eq. (4) independent of β_2. On the other hand, significant ground-state deformation of $\beta_2 \approx 0.25$ is found for the residues ^{115,119}Te populated in the other two reactions. The β_2 values were estimated from the calculated total-Routhain-surface (TRS) in the macroscopic-microscopic model using Woods Saxon potential and Strutinsky shell correction approach [46].

Apart from the NLD, the HF model also requires transmission coefficients to estimate the statistical decay widths for different evaporation channels. These coefficients were calculated using the optical model (OM), where model parameters for neutron, proton [47], and α [48] were taken appropriately. We observed that the variations in the OM parameters have negligible effect in deciding the spectral shape; whereas it is mainly governed by the NLD parameter a. Further, to reproduce the measured data, the calculated spectra were needed to be scaled down by a constant factor. This factor was determined by normalizing the calculated spectra with the measured data at the peak position. However no scaling is required for the spectrum of ^{4}He + ^{112}Sn calculated using Eq. (3). This trivial scaling procedure does not alter the shapes of neutron energy spectra.

4.2. Isolating different evaporation channels

Calculated inclusive neutron spectra and the partial contributions of different evaporation channels are shown in Fig. 2 for each individual reactions at the lowest E^*_{CN}. For the present reactions, the relevant evaporation channels are: one ($1n$), two ($2n$), three ($3n$) neutrons, proton followed by neutron (pn), and α followed by neutron (αn). Relative contributions of different channels depend on the nuclear mass, charge, and E^*_{CN}. Here, we simply use Eq. (1) in the BSFG model to identify relative contributions of neutrons from different decay channels. Fig. 2 illustrates that, the majority (> 90%) of the evaporated neutrons come from the $1n$-channel for neutron energies $E_n > 2.5$ MeV in ^{4}He + ^{112}Sn, ^{116}Sn and $E_n > 5.5$ MeV in ^{4}He + ^{124}Sn respectively. Contributions of other channels are only visible below these E_n limits, say E^1_n. The values of E^1_n however slightly depend on the choice of the formula used for the $\tilde{a}$, and these are adjusted accordingly to include only the $1n$-channel in the subsequent analysis.

4.3. Validation of different parametrizations of $\tilde{a}$

Measured neutron energy spectra corresponding to the three reactions (Te residues) are compared with the theoretical spectra obtained using four different formulae of NLD parameter $\tilde{a}$ as given in Eqs. (1), (2), (3), and (4) and are shown in Fig. 3. Figs. 3(a)-(c) show that, irrespective of the choice of reaction (Te isotope), Eq. (3) or the explicit $(Z - Z_0)$ dependence provides the best overall match in comparison to the other three prescriptions. This is also reflected in the ratio plot [see Fig. 3(d)-(e)] generated by dividing the measured data with the calculated spectra. Even though Eq. (4) takes the deformation effects into account, it fails to predict the data for the two strongly-deformed isotopes. Moreover, as both $(N - Z)$ and $(Z - Z_0)$ vary considerably (see Table 1) among the different reactions, our conclusion on the stronger $(Z - Z_0)$ dependency with respect to $(N - Z)$ is quite unambiguous. Above conclusion is also not altered by any possible pre-equilibrium contamination as the calculated distribution considering compound + pre-equilibrium decay fail to reproduce the measured data [see dashed lines in Figs. 3(a)-(c)].

The values of shell corrected NLD parameter a for the most significant residue nuclei in the three cases resulting from the $(Z - Z_0)$ formula are tabulated in Table 1. Evidently, NLD parameter a decreases for the two isotopes located away from the β-stability line. The rate of reduction is sharper than that predicted by the global systematics [49] (see Table 1); the best agreement with the systematics being found for the heaviest isotope.

Next, we investigate the robustness of our conclusion at higher E^*_{CN}. In general, α [see Eq. (1)] may vary with E^*_{CN}. Therefore, we

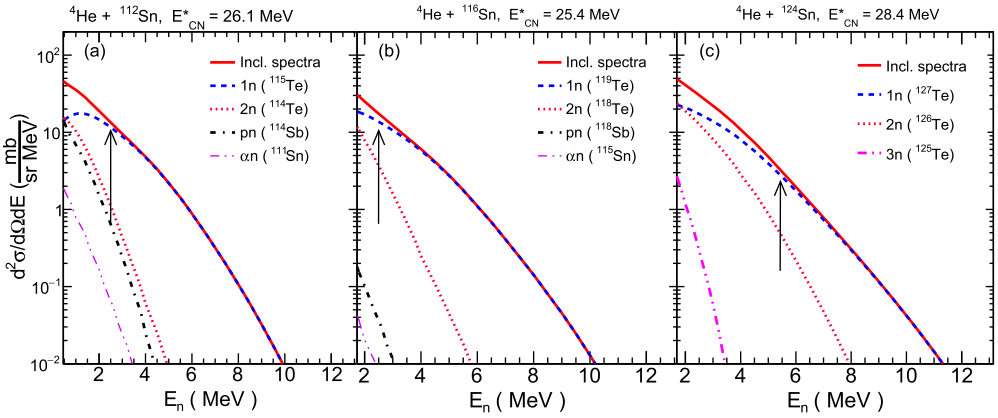

Fig. 2. Calculated neutron energy spectra from different evaporation channels along with the total spectra for ^{4}He + ^{112,116,124}Sn are shown in panels (a), (b), and (c). The dominance (> 90%) of *1n*-channel is found to be obvious for the three systems, whose initial energy ranges are indicated by arrows.

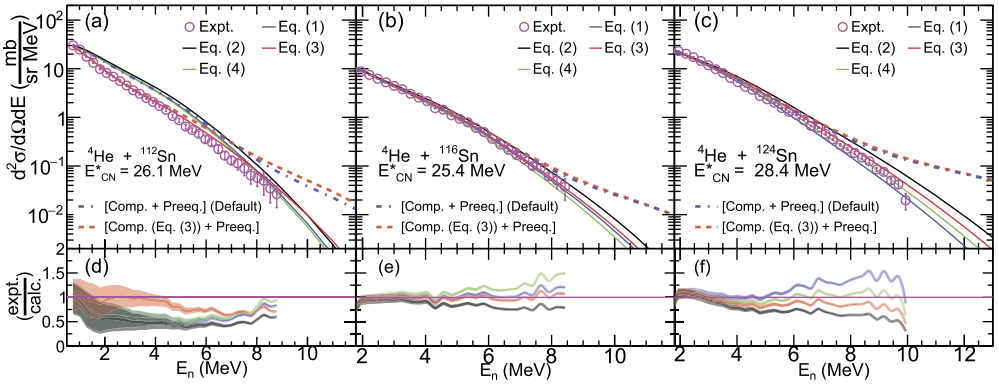

Fig. 3. Panels (a), (b) and (c) show experimental data for ^{4}He + ^{112,116,124}Sn in symbols. The calculated spectra considering compound nuclear decay with NLD estimated using BSFG model for four different formalism of NLD parameter [Eqs. (1)-(4)] are shown in solid lines. Excitation energy of the corresponding compound nuclei formed in these reactions are mentioned in the figure. Calculated spectra considering compound + pre-equilibrium decay are shown in dashed line; one with Talys default parameters and another with Eqn. (3) for compound nuclear decay and Talys default for pre-equilibrium. Calculated spectra shown in panels (a), (b), and (c) are scaled down by factors of 1.35, 2.8, and 2.0, respectively (see text). No such factor is used for calculated spectra using Eq. (3) in ^{112}Sn. Panels (d), (e) and (f) show ratio plots between the measured data and the spectra calculated for compound nuclear decay using different formalisms of NLD parameter. Shaded regions indicate the uncertainty in the ratio. Magenta line passed through the centre on y-axis is for reference.

Table 1
Ground state quadrupole deformation β_2, neutron separation energy S_n, $(N-Z)$ and $(Z-Z_0)$ are shown for the dominant evaporation residues formed in the ^{4}He + ^{112,116,124}Sn reactions. S_n^P is the neutron separation energy of the parent nucleus. Shell corrected NLD parameters a and NLDs at S_n for the three different residues are also shown.

Nucleus populated	β_2	S_n (MeV)	S_n^P [see text] (MeV)	$(N-Z)$	$(\lvert Z-Z_0\rvert)$	a present work (MeV^{-1})	a Ref. [49] (MeV^{-1})	$\rho(S_n)$ expt. [sysm.] (MeV^{-1})
^{115}Te	0.25	8.24	11.27	11	2.5	11.291	12.182	6.21×10^5 (estm.)
^{119}Te	0.24	7.56	10.25	15	1.0	14.378	13.223	6.41×10^5 (estm.)
^{127}Te	0.08	6.29	8.78	23	2.1	12.281	12.243	5.87×10^4 (expt. D_0)

refit α for different E^*_{CN} of the reference nucleus (^{119}Te); this does not perturb the general conclusion on $\tilde{a}$ discussed above. In fact, E^*_{CN}s of the three isotopes do not exactly overlap. Accordingly, we interpolate α to eliminate possible discrepancies arising from this energy mismatch. We find that the observed nature of $\tilde{a}$ expressed by Eq. (3) remains to be the best option even at higher beam energies. To demonstrate this, we determined the inclusive differential cross-section $(d\sigma/d\Omega)_{150^\circ}$ of neutron-evaporation at 150° by integrating the neutron spectra over the whole E_n range to taken into account all the possible evaporation channels. For higher E^*_{CN}, we can not restrict the analysis to the *1n*-channel only as its contribution to the total spectra reduces drastically with the increase in energy. Calculated $(d\sigma/d\Omega)_{150^\circ}$ are compared in Fig. 4 with our measured data for different $E_{c.m.}$. A better agreement, especially for the ^{4}He+^{112}Sn reaction, can be observed when Eq. (3) is used to estimate the NLD parameter $\tilde{a}$.

5. Determination of nuclear level density

The backward angle neutron spectra measured at the lowest beam energy were used to extract NLDs of the residual nuclei, ^{115,119,127}Te populated in three reactions. To this end, we employ the following scaling relation [50]:

$$\rho_{\rm exp}(E^*) = \rho_{\rm model}(E^*)\frac{(d\sigma/dE_n)_{\rm exp}}{(d\sigma/dE_n)_{\rm model}}. \quad (5)$$

Here, the excitation energy of the residue (E^*) is determined from the corresponding E^*_{CN}, since $E^* = E^*_{CN} - S_n^P - E_n$; S_n^P being the neutron separation energy of the parent nucleus as given in Table 1. The $\rho_{\rm model}$ and the associated cross sections were calculated using the BSFG model [Eq. (A.1)] where Eq. (3) was used to calculate $\tilde{a}$. NLDs were extracted only using the part of the spectra for

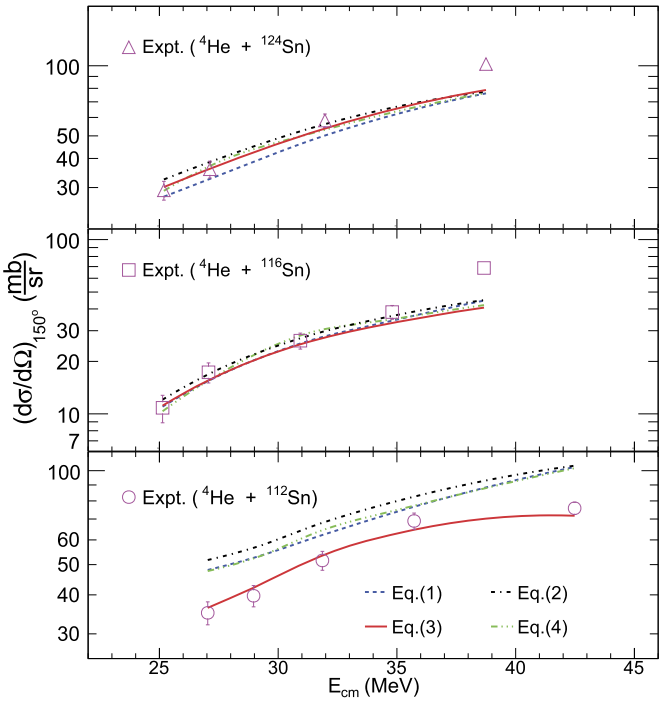

Fig. 4. Measured $d\sigma/d\Omega$ at 150° plotted as a function of centre-of-mass energy E_{cm} are shown in symbols. Lines represent calculated differential cross sections considering all neutron evaporation channels. Calculations are done using different formulae of NLD parameter described in Eqs. (1)-(4). Calculated cross sections are scaled down by the same factors as used in Fig. 3(a)-(c).

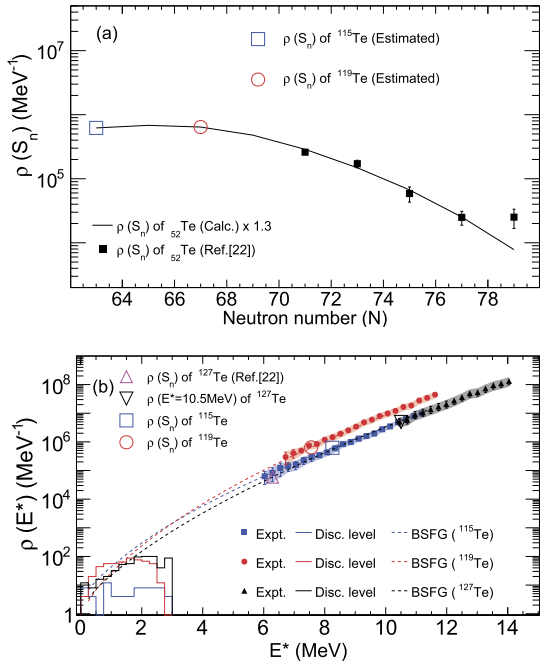

Fig. 5. Panel (a) shows the NLDs at S_n for different Te-isotopes determined from the experimental D_0 values (solid square), and the calculated NLDs (solid line) using BSFG model (see text). Symbols in open square and open circle are the estimated $\rho(S_n)$ for ^{115}Te and ^{119}Te, respectively. Panel (b) shows the measured nuclear level densities for ^{115,119,127}Te as function of residue excitation energies, which are normalized at the respective neutron separation energies (see text). Shaded regions are the uncertainties in NLDs (see text). Solid line histograms are the NLDs obtained from the known discrete energy levels and dashed lines are the BSFG model calculations.

which $E_n > E_n^1$. Since Eq. (5) alone cannot determine the absolute values of NLD [20]. The measured NLDs were further normalized with respect to $\rho(S_n)$, which was determined in absolute scale at $E^* = S_n$.

For ^{127}Te, $\rho(S_n)$ was extracted from the experimental average neutron resonance spacing D_0 [22] measured at $E^* = S_n$. Corresponding relation [Eq. (A.4)] is given in the Appendix. Unfortunately, measured D_0 values are not available for ^{115,119}Te. Therefore, we obtain $\rho(S_n)$ of these two isotopes using the following procedure. First, $\rho(S_n)$s were calculated from Eq. (A.4) for all the odd-mass Te isotopes for which the experimental D_0 values are available. These are plotted in Fig. 5(a) as a function of the neutron number. Then, we recalculate these $\rho(S_n)$ by using the BSFG model with the parameters taken from the global systematics [49]. It is observed [see Fig. 5(a)] that the BSFG model could nicely reproduce the general trend of experimental $\rho(S_n)$ when multiplied by a factor of 1.3. Finally, we obtain $\rho(S_n)$ for ^{115,119}Te by extrapolating the same BSFG calculation to the respective masses. This is demonstrated in Fig. 5(a) and the extracted values of $\rho(S_n)$ are mentioned in Table 1. For ^{127}Te, since the initial E^* is higher than S_n, an additional normalization at E^* = 10.5 MeV was done by determining $\rho(10.5MeV)$ using the same procedure as described for ^{115,119}Te.

The normalized $\rho_{\exp}(E^*)$ for the three isotopes are plotted as a function of E^* in Fig. 5(b). Transparent shaded regions are the uncertainties in NLDs incorporating systematic as well as statistical uncertainties. Detail procedure for the estimation of uncertainties are described in the appendix. An extrapolation of the measured NLDs down to the lower E^* are obtained using BSFG calculation shown in dashed line. Extrapolated NLDs match quite nicely at $E^* \sim$ 1.5 MeV with the same obtained from the known discrete levels [51] except for ^{115}Te.

It can be seen that the measured NLDs of ^{115,127}Te at any E^* are lesser than the NLD of ^{119}Te. Precisely, at E^* = 10.5 MeV, the NLDs of ^{115,127}Te is lower by a factor of 3 in comparison to that of ^{119}Te. Although the reduction factor may change due to uncertainty in the D_0 estimation for ^{115,119}Te, but the general trend is established independently from the analysis of the neutron energy spectra itself where the data for all the isotopes could only be explained simultaneously using the $(Z - Z_0)$ form of the NLD parameter. It is also important to mention here that, the reduction of NLD in ^{115,127}Te in comparison to ^{119}Te is not due to the deformation driven collective enhancement otherwise the change in NLD for ^{115,127}Te would be in opposite direction. More experimental data for a range of isotopes in different mass regions are required to validate the isospin dependent prescriptions of the NLD parameter on the global mass range.

6. Conclusions

A systematic study is performed to understand the $(N - Z)$ asymmetry dependence on the nuclear level density by measuring the emitted neutrons from ^{4}He + ^{112,116,124}Sn reactions in the excitation energy range of 25-42 MeV. Measured neutron energy spectra are compared with the statistical model calculation including the isospin dependent and independent prescriptions of level density parameter. Among the available formalism, the isospin dependent prescription in the form of $(Z - Z_0)$ is found to be most suitable in reproducing the measured spectra for all the three reactions. Further, nuclear level densities determined from the measured neutrons spectra show a reduction for ^{115,127}Te in comparison to that of ^{119}Te, which lies closer to the beta stability line. Such kind of experimental results on isospin dependence of nuclear level density has been unveiled for the first time in a range of isotopes with $A >$110.

Declaration of competing interest

The authors declare that they have no known competing financial interests or personal relationships that could have appeared to influence the work reported in this paper.

Acknowledgements

The authors would like acknowledge the VECC Cyclotron operators for smooth running of the accelerator during the experiment. We like to thank Partha Dhara for his assistance with the data acquisition system. We also like to thank Jaikiran Meena, Ruchismita Mondal saha, Amiya Kumar Saha, Jayanta Kumar Sahoo for their help during experimental setup. Two of the authors (R. Shil and A. Chakraborty) would like to thank UGC-DAE CSR, Kolkata for providing financial support through the CRS project (Project Sanction No. UGC-DAE-CSR-KC/CRS/19/NP10/0921/0963). One of the authors (S. Bhattacharya) acknowledges with thanks the financial support received as Raja Ramanna Fellow from the Department of Atomic Energy, Government of India.

Appendix A

Level density expression $\rho(E^*)$ at excitation energy E^* following Back-shifted Fermi Gas model [45] can be expressed as

$$\rho(E^*) = \frac{1}{12\sqrt{2}\sigma}\frac{\exp 2\sqrt{a(E^*-\Delta)}}{a^{1/4}(E^*-\Delta)^{5/4}}, \tag{A.1}$$

where a is the level density parameter, Δ is an empirical parameter related to the pairing energy and σ is the spin cutoff parameter. NLD parameter a depends on the excitation energy which can be written as $a(U) = \tilde{a}[1 + \frac{\Delta S}{U}(1 - \exp(-\gamma U))]$ [8] where $U = E^* - \Delta$ and $\tilde{a}$ is the asymptotic value of level density parameter. ΔS is the ground state shell correction energy which is taken from Ref. [52]. Parameter γ determines the rate at which the shell effect is depleted with the increase in excitation energy which is taken from Ref. [21].

The value of Δ is estimated as $\chi(12/\sqrt{A}) + \delta$ [21]. Here χ = -1, 0, 1 for odd-odd, odd-even, even-even nucleus, δ is the additional pairing energy shift with a global constant value 0.17301 and A is the nuclear mass. Sensitivity of Δ in the determination of NLD parameter a has been checked by varying Δ from its calculated value by 20%. The resultant variation in a was found to be negligible for the studied system.

The value of σ can be calculated using any of the five different models available in the literature [21,49,53,54]. However these values vary to a large extent e.g. for ^{119}Te, the values lie between 4.31 [49] and 6.03 [53]. Therefore the range of σ values were determined for each nucleus and NLDs were calculated using middle of the σ range [55]. The deviation of this value from the two extremes were used to determine the systematic uncertainty in NLD. Total uncertainties are obtained by adding in quadrature the statistical and systematic uncertainties.

For isobaric nuclei having mass A, the atomic number Z_0 of the beta stable nucleus can be estimated using the following relation [29]

$$Z_0 = \frac{0.5042A}{1 + 0.0073A^{2/3}}. \tag{A.2}$$

The coefficients B_s and B_k, as described in Eq. (4) [12], can be determined from the value of nuclear deformation parameter (β_2) using the following relations:

$$B_s = 1 + \frac{\beta_2^2}{2\pi} - \sqrt{\frac{5}{1764\pi^3}}\beta_2^3 - \frac{33}{56\pi^2}\beta_2^4$$

$$B_k = 1 + \frac{\beta_2^2}{2\pi} + \sqrt{\frac{20}{441\pi^3}}\beta_2^3 - \frac{41}{56\pi^2}\beta_2^4 \tag{A.3}$$

The level density at the neutron separation energy can be determined using the experimental average neutron resonance spacing (D_0) as per the following relation [56]:

$$\rho_0(S_n) = \frac{2\sigma^2}{D_0}[(I_t+1)\exp\frac{-(I_t+1)^2}{2\sigma^2} + I_t\exp\frac{-I_t^2}{2\sigma^2}]^{-1}. \tag{A.4}$$

Here, I_t is the spin of the target nucleus and σ can be determined using the parametrization of Ref. [49].

References

[1] Till Von Egidy, Dorel Bucurescu, Phys. Rev. C 72 (2005) 044311.
[2] R.J. Charity, L.G. Sobotka, J.F. Dempsey, M. Devlin, S. Komarov, D.G. Sarantites, A.L. Caraley, R.T. deSouza, W. Loveland, D. Peterson, B.B. Back, C.N. Davids, D. Seweryniak, Phys. Rev. C 67 (2003) 044611.
[3] S. Hilaire, Phys. Lett. B 583 (2004) 264.
[4] R.J. Charity, Phys. Rev. C 82 (2010) 014610.
[5] P. Roy, S. Mukhopadhyay, M. Aggarwal, D. Pandit, T.K. Rana, S. Kundu, T.K. Ghosh, K. Banerjee, G. Mukherjee, S. Manna, A. Sen, R. Pandey, D. Mondal, S. Pal, D. Paul, K. Atreya, C. Bhattacharya, Phys. Rev. C 103 (2021) 024602.
[6] Y.K. Gupta, B. John, D.C. Biswas, B.K. Nayak, A. Saxena, R.K. Choudhury, Phys. Rev. C 78 (2008) 054609.
[7] K. Banerjee, S. Bhattacharya, C. Bhattacharya, M. Gohil, S. Kundu, T.K. Rana, G. Mukherjee, R. Pandey, P. Roy, H. Pai, A. Dey, T.K. Ghosh, J.K. Meena, S. Mukhopadhyay, D. Pandit, S. Pal, S.R. Banerjee, Phys. Rev. C 85 (2012) 064310.
[8] A.V. Ignatyuk, G.N. Smirenkin, A.S. Tishin, Sov. J. Nucl. Phys. 21 (1975) 255.
[9] S.K. Kataria, V.S. Ramamurthy, S.S. Kapoor, Phys. Rev. C 18 (1978) 549.
[10] P. Roy, K. Banerjee, C. Bhattacharya, R. Pandey, A. Sen, S. Manna, S. Kundu, T.K. Rana, T.K. Ghosh, G. Mukherjee, T. Roy, A. Dhal, A. Dey, J.K. Meena, A.K. Saha, D. Pandit, S. Mukhopadhyay, S. Bhattacharya, Phys. Rev. C 94 (2016) 064607.
[11] A.V. Ignatyuk, K.K. Istekov, G.N. Smirenkin, Sov. J. Nucl. Phys. 29 (1979) 450.
[12] W. Reisdorf, Z. Phys. A 300 (1981) 227.
[13] P. Roy, K. Banerjee, M. Gohil, C. Bhattacharya, S. Kundu, T.K. Rana, T.K. Ghosh, G. Mukherjee, R. Pandey, H. Pai, V. Srivastava, J.K. Meena, S.R. Banerjee, S. Mukhopadhyay, D. Pandit, S. Pal, S. Bhattacharya, Phys. Rev. C 88 (2013) 031601(R).
[14] K. Banerjee, P. Roy, D. Pandit, J. Sadhukhan, S. Bhattacharya, C. Bhattacharya, G. Mukherjee, T. Ghosh, S. Kundu, A. Sen, T.K. Rana, S. Manna, R. Pandey, T. Roy, A. Dhal, M. Asgar, S. Mukhopadhyay, Phys. Lett. B 772 (2017) 105.
[15] D. Pandit, S. Bhattacharya, D. Mondal, P. Roy, K. Banerjee, S. Mukhopadhyay, S. Pal, A. De, B. Dey, S.R. Banerjee, Phys. Rev. C 97 (2018) 041301(R).
[16] S.M. Grimes, T.N. Massey, A.V. Voinov, Phys. Rev. C 99 (2019) 064331.
[17] G. Mohanto, A. Parihari, P.C. Rout, S. De, E.T. Mirgule, B. Srinivasan, K. Mahata, S.P. Behera, M. Kushwaha, D. Sarkar, B.K. Nayak, A. Saxena, A.K. Rhine Kumar, A. Gandhi Sangeeta, Nabendu K. Deb, P. Arumugam, Phys. Rev. C 100 (2019) 011602(R).
[18] M. Guttormsen, et al., Phys. Lett. B 816 (2021) 136206.
[19] Y. Alhassid, G.F. Bertsch, S. Liu, H. Nakada, Phys. Rev. Lett. 84 (2000) 4313.
[20] P. Roy, K. Banerjee, T.K. Rana, S. Kundu, D. Pandit, N. Quang Hung, T.K. Ghosh, S. Mukhopadhyay, D. Mondal, G. Mukherjee, S. Manna, A. Sen, S. Pal, R. Pandey, D. Paul, K. Atreya, C. Bhattacharya, Eur. Phys. J. A 57 (2021) 48.
[21] R. Capote, et al., Nucl. Data Sheets 110 (2009) 3107.
[22] RIPL-3 Reference Input Parameter Library for calculations of Nuclear Reactions and Nuclear Data Evaluation; available at http://www-nds.iaea.org/RIPL-3/.
[23] A. Schiller, L. Bergholt, M. Guttormsen, E. Melby, J. Rekstad, S. Siem, Nucl. Instrum. Methods Phys. Res., Sect. A 447 (2000) 498.
[24] M. Guttormsen, et al., Eur. Phys. J. A 51 (2015) 170.
[25] A. Spyrou, S.N. Liddick, A.C. Larsen, M. Guttormsen, K. Cooper, A.C. Dombos, D.J. Morrissey, F. Naqvi, G. Perdikakis, S.J. Quinn, T. Renstrøm, J.A. Rodriguez, A. Simon, C.S. Sumithrarachchi, R.G.T. Zegers, Phys. Rev. Lett. 113 (2014) 232502.
[26] A.V. Voinov, S.M. Grimes, U. Agvaanluvsan, E. Algin, T. Belgya, C.R. Brune, M. Guttormsen, M.J. Hornish, T. Massey, G.E. Mitchell, J. Rekstad, A. Schiller, S. Siem, Phys. Rev. C 74 (2006) 014314.
[27] A.S. Jensen, Phys. Lett. B 105 (1977) 68.
[28] S.I. Al-Quraishi, S.M. Grimes, T.N. Massey, D.A. Resler, Phys. Rev. C 63 (2001) 065803.
[29] S.I. Al-Quraishi, S.M. Grimes, T.N. Massey, D.A. Resler, Phys. Rev. C 67 (2003) 015803.
[30] H. Nakada, Y. Alhassid, Phys. Rev. C 78 (2008) 051304(R).
[31] R.J. Charity, L.G. Sobotka, Phys. Rev. C 71 (2005) 024310.
[32] R. Moro, A. Brondi, N. Gelli, M. Barbui, A. Boiano, M. Cinausero, A. Di Nitto, D. Fabris, E. Fioretto, G. La Rana, F. Lucarelli, M. Lunardon, G. Montagnoli, A. Ordine, G. Prete, V. Rizzi, M. Trotta, E. Vardaci, Eur. Phys. J. A 48 (2012) 159.

[33] A.V. Voinov, T. Renstrøm, D.L. Bleuel, S.M. Grimes, M. Guttormsen, A.C. Larsen, S.N. Liddick, G. Perdikakis, A. Spyrou, S. Akhtar, N. Alanazi, K. Brandenburg, C.R. Brune, T.W. Danley, S. Dhakal, P. Gastis, R. Giri, T.N. Massey, Z. Meisel, S. Nikas, S.N. Paneru, C.E. Parker, A.L. Richard, Phys. Rev. C 99 (2019) 054609.
[34] G.K. Prajapati, Y.K. Gupta, B.V. John, B.N. Joshi, Harjeet Kaur, Nishant Kumar, L.S. Danu, S. Mukhopadhyay, S. Dubey, S.R. Jain, D.C. Biswas, B.K. Nayak, Phys. Rev. C 102 (2020) 054605.
[35] P. Roy, K. Banerjee, T.K. Rana, S. Kundu, S. Manna, A. Sen, D. Mondal, J. Sadhukhan, M.T. Senthil Kannan, T.K. Ghosh, S. Mukhopadhyay, D. Pandit, G. Mukherjee, S. Pal, D. Paul, K. Atreya, C. Bhattacharya, Phys. Rev. C 102 (2020) 061601(R).
[36] H.A. Bethe, Phys. Rev. 50 (1936) 332;
H.A. Bethe, Rev. Mod. Phys. 9 (1937) 69.
[37] D. Pandit, S. Mukhopadhyay, S. Bhattacharya, S. Pal, A. De, S.R. Banerjee, Nucl. Instrum. Methods Phys. Res., Sect. A 624 (2010) 148.
[38] K. Banerjee, T.K. Ghosh, S. Kundu, T.K. Rana, C. Bhattacharya, J.K. Meena, G. Mukherjee, P. Mali, D. Gupta, S. Mukhopadhyay, D. Pandit, S.R. Banerjee, S. Bhattacharya, T. Bandyopadhyay, S. Chatterjee, Nucl. Instrum. Methods Phys. Res., Sect. A 608 (2009) 440.
[39] S. Chatterjee, K. Banerjee, D. Pandit, P. Roy, T. Bandyopadhyay, R. Ravishankar, C. Bhattacharya, S. Bhattacharya, D. Datta, S.R. Banerjee, Appl. Radiat. Isot. 128 (2017) 216.
[40] A.S. Roy, K. Banerjee, P. Roy, S. Seth, T.K. Rana, A. Sen, D. Pandit, S. Kundu, T.K. Ghosh, G. Mukherjee, S. Manna, R. Pandey, D. Paul, K. Atreya, S. Basu, V. Suman, P.C. Rout, T. Santhosh, S. Mukhopadhyay, D. Mondal, S. Pal, S. Saha, M. Das, R. Ravishankar, M.S. Kulkarni, S. Pal, C. Bhattacharya, J. Instrum. 16 (2021) P07045.
[41] A.J. Koning, S. Hilaire, M.C. Duijvestijn, TALYS-1.8, available at https://www.talys.eu.
[42] A.J. Koning, M.C. Duijvestijn, Nucl. Phys. A 744 (2004) 15.
[43] H. Gruppelaar, P. Nagel, P.E. Hodgson, Riv. Nuovo Cimento 7 (1986) 1.
[44] W. Hauser, H. Feshbach, Phys. Rev. 87 (1952) 366.
[45] W. Dilg, W. Schantl, H. Vonach, M. Uhl, Nucl. Phys. A 217 (1973) 269.
[46] G. Mukherjee, P. Joshi, R.K. Bhowmik, S.N. Roy, S. Dutta, S. Muralithar, R.P. Singh, Nucl. Phys. A 829 (2009) 137 and references therein.
[47] A.J. Koning, J.P. Delaroche, Nucl. Phys. A 713 (2003) 231.
[48] S. Watanabe, Nucl. Phys. 8 (1958) 484.
[49] T. von Egidy, D. Bucurescu, Phys. Rev. C 80 (2009) 054310.
[50] H. Vonach, Proceedings of the IAEA Advisory Group Meeting on Basic and Applied Problems of Nuclear Level Densities, Upton, New York, 1983, Brookhaven National Laboratory Report No. BNL-NCS-51694, 1983, p. 247.
[51] Brookhaven National Laboratory, National Nuclear Data Center online data service, http://www.nndc.bnl.gov.
[52] W.D. Myers, W.J. Swiatecki, Lawrence Berkeley Laboratory Report No. LBL-36803, 1994.
[53] U. Facchini, E. Saetta-Menichella, Nucl. Energy (Milan) 15 (1967) 54.
[54] S.M. Grimes, J.D. Anderson, J.W. McClure, B.A. Pohl, C. Wong, Phys. Rev. C 10 (1974) 2373.
[55] S.N. Liddick, et al., Phys. Rev. C 100 (2019) 024624.
[56] H.K. Toft, A.C. Larsen, U. Agvaanluvsan, et al., Phys. Rev. C 81 (2010) 064311.